Biochimica et Biophysica Acta, 1015 (1990) 131–140
Elsevier

BBABIO 43113

Formation by NO of nitrosyl adducts of redox components of the Photosystem II reaction center. I. NO binds to the acceptor-side non-heme iron

Vasili Petrouleas [1] and Bruce A. Diner [2]

[1] *Institute of Materials Science, Nuclear Research Center, 'Demokritos', Aghia Paraskevi, Attiki (Greece)*
[2] *Central Research and Development Department, E.I. DuPont de Nemours Co., Wilmington, DE (U.S.A.)*

(Received 14 April 1989)
(Revised manuscript received 29 August 1989)

Key words: Photosystem II reaction center; Nitric oxide; Non-heme iron; ESR; Mossbauer; Quinone-iron complex

NO is a good electrophile and EPR spin probe, carrying an unpaired electron ($S = 1/2$). Exposure of Photosystem II reaction centers to NO results in the appearance of an EPR signal at $g = 4$. Dark titration with NO shows a $K_d \approx 30$ μM in spinach chloroplasts and 250 μM in BBY preparations. Successive cycles of illumination at 200 K, followed by incubation at 245 K, results in binary oscillations of the amplitude of the $g = 4$ signal in spinach chloroplasts. This signal is small in states $Q_A^- Q_B$, $Q_A^- Q_B^-$ and $Q_A Q_B^-$, but large in states $Q_A Q_B$ and $Q_A Q_B H_2$ of the PS II acceptor side. NO slows electron transfer between Q_A and Q_B (Diner, B.A and Petrouleas, V. (1990) Biochim. Biophys. Acta 1015, 141–149) and modifies the Mössbauer spectrum of the non-heme Fe(II). These results strongly support the assignment of the $g = 4$ EPR signal to an acceptor side Fe(II)-NO adduct in an $S = 3/2$ state. Exchange coupling of this species with the $S = 1/2$ semiquinones results in an integral spin system, not detectable in X-band EPR. The $g = 4$ spectrum can be described by a spin hamiltonian. The rhombicity parameter E/D is in all cases small ($\leqslant 0.015$), implying a near axial environment. NO can donate electrons to PS II. Charge recombination, following a light flash in the presence of DCMU, is blocked by NO ($K_m \approx 30$ μM, 25 °C). NO also reacts reversibly in the dark with D^+ (an oxidized secondary donor), resulting in the disappearance of Signal II_{dark} with a K_d of 3 μM. Pumping off of NO in the dark results in full recovery of the signal.

Introduction

The environment of the non-heme iron of the quinone-iron complex of Photosystem II (PS II) is thought to closely resemble that of the reaction centers of the purple non-sulfur photosynthetic bacteria. EPR [1–4] and Mössbauer [5–7] spectra suggest similar ligands and symmetries for the iron coordination and would locate the iron at a similar distance (approx. 7 Å, [8–10]) from each of the quinone electron acceptors, Q_A and Q_B. Comparison of the primary structure of the polypeptides implicated in the coordination of the primary photoreactants [11–14] show that the D1 and D2 polypeptides of PS II contain two histidines each in positions homologous to the L and M histidines of the bacterial reaction centers which coordinate the iron. While it has been suggested that the M232 glutamic acid homologue may be missing in PS II [14], there are several carboxylic amino acids in the hydrophilic loop connecting helices IV and V of polypeptides D1 and D2 which could serve such a function.

There are differences, however, in the redox and spectroscopic behavior of the non-heme iron in the two types of reaction center. The iron of PS II clearly has a lower midpoint potential for the Fe(II)/Fe(III) redox couple ($E_{m,7} = 400$ mV) [15]. Attempts [16,17] at oxidation of the Fe(II) in reaction centers of two bacterial species (*Rb. sphaeroides* and *R. rubrum*) have been unsuccessful, implying that the midpoint potential in these centers is probably greater than 550 mV. The

Abbreviations: BBY, Berthold, Babcock, Yocum [29]; D, a tyrosine acting as a secondary electron donor in the PS II reaction center [47–49]; DCMU, diuron (3-(3,4-dichlorophenyl)-1,1-dimethylurea); DMSO, dimethylsulfoxide; EPR, Electron paramagnetic resonance; Hepes, (4-(2-hydroxyethyl)-1-piperazineethanesulfonic acid; Mes; 4-morpholinethanesulfonic acid; PS I-Photosystem I; PS II, Photosystem II; Q_A, primary quinone electron acceptor of PS II; Q_B, secondary quinone electron acceptor of PS II.

Correspondence: V. Petrouleas, Institute of Materials Science, Nuclear Research Center, 'Demokritos', 15310 Aghia, Paraskevi, Attiki, Greece.

Q_A^--Fe(II) EPR signal of PS II shows an interconversion between two alternate resonance forms as a function of pH [4] and the Fe(II) Mössbauer spectrum of PS II shows a heterogeneity in the quadrupole splittings [17], implying that the symmetry and ligands to the iron do not assume a unique configuration in this reaction center.

In the course of this paper and the one that follows [18], we will show that the non-heme iron of PS II has a reactive coordination position. This position can be occupied by both natural and artificial ligands. We demonstrate here for the first time the ability to form reversible nitrosyl complexes of the PS II Fe(II). NO is known to readily form adducts with non-heme Fe(II) coordination complexes, in many cases formally described as an $S = 3/2$ ($3d^7$) system which gives characteristic EPR signals at $g = 4$ [19–25]. This signal has been used to great advantage as a probe in the study of a number of dioxygenases [20,21] and of soybean lipoxygenase [22,23]. These results are of particular interest for comparison with the present case as the Mössbauer spectrum of PS II Fe(II) [6,7] and the EPR spectrum of Fe(III) [15] show many features in common with the non-heme iron of a number of dioxygenases [20] and soybean lipoxygenase [26].

It will also be demonstrated that NO interacts reversibly with components on the PS II donor side.

Materials and Methods

Photosynthetic membranes

Thylakoid membrane fragments (BBY membranes) were prepared from market spinach with some modification [27,28] of the original procedure [29]. After the final centrifugation step, the membranes were resuspended at 10–15 mg Chl/ml in 5 mM Mes-NaOH (pH 6.5), 15 mM NaCl, 5 mM $MgCl_2$ and 0.4 M sucrose, frozen rapidly in liquid nitrogen and stored in liquid nitrogen until use.

Membranes were prepared from *Scenedesmus* wild-type and LF-1 mutant [30] according to Metz and Seibert [31] with resuspension in 50 mM sodium phosphate (pH 6.9), 0.3 M sucrose and 50 mM NaCl.

Chloroplasts were prepared according to Avron [32] from spinach grown in growth chambers. Chloroplasts were resuspended in 50 mM Tris-HCl (pH 7.5) containing 10 mM NaCl, 0.4 M sucrose ml 5% DMSO, and stored at −80 °C.

Chlamydomonas PS II core preparations were prepared according to Diner and Wollman [33].

Electron spin resonance and Mössbauer spectroscopy

Electron spin resonance spectra were obtained using a Bruker ER 200D-SRC spectrometer equipped with an Oxford ESR 9 cryostat [15]. Measurement conditions were as as described in the figure legends.

Illumination of samples in EPR tubes (3 mm inner diameter) was carried out in a transparent dewar containing a liquid-frozen acetone bath (200 K). Light was provided by a 360 W projector lamp, filtered by a 1.5 cm thick bath of saturated $CuSO_4$. During illumination for a total of 3 min (four 90° rotations, 45 s each position), the sample temperature did not exceed 220 K.

Mössbauer measurements were obtained using a constant acceleration spectrometer and a $^{57}Co(Rh)$ source.

Fluorescence relaxation kinetics

A flash-detection spectrophotometer similar to that designed by Joliot et al. [34] was used in the fluorescence detection mode. A saturating actinic xenon flash was filtered by an infrared reflecting filter (Athervex TA2, MTO) and a Corning 4-96. The fluorescence yield was detected using a probe flash at 422 nm spaced at various times after the actinic flash. The chlorophyll fluorescence was filtered through a set of blocking filters – Schott KV550, Ulano Rubylith, Corning 2-64, and a Kodak Wratten 70 transmitting above 670 nm.

NO treatment

Anaerobic conditions are required for handling NO, as it readily reacts with O_2 to form NO_2. Samples for EPR spectroscopy were slowly bubbled inside the EPR tube with known mixtures of NO and N_2 using an airtight syringe. Samples for fluorescence studies were prepared by diluting chloroplasts 400-fold in buffer, previously flushed with N_2 in an air-tight vial. Aliquots of a saturated solution of NO (3.3 mM at 0 °C) were added to give the desired NO concentration.

Results

Effect of NO on the PS II electron acceptor side

An NO-induced $g = 4$ EPR signal in BBY membranes

Fig. 1 (dotted trace) shows the $g = 4$ region of the EPR spectrum of an untreated BBY spinach preparation at pH 6.0. Apart from the iron impurity peak at $g = 4.29$ attributed to adventitious rhombic Fe(III), there are no other features apparent. Treatment with 0.8 mM NO in the dark at 4 °C elicits a strong signal (Fig. 1, continuous line) which consists of closely spaced absorption and derivative-like contributions with an average g-value of 4. A similar signal has been observed in a number of dioxygenases [20,21], as well as in Fe(II)-EDTA and soybean lipoxygenase [22,23] treated with NO, and has been attributed to an Fe(II)-NO complex. As in the above examples, removal of NO by bubbling with N_2 or by pumping, dramatically decreases the amplitude of the $g = 4$ signal. In the case of PS II, the $g = 4$ signal can also be made to disappear reversibly by illumination at cryogenic temperatures. Fig. 1 (dashed

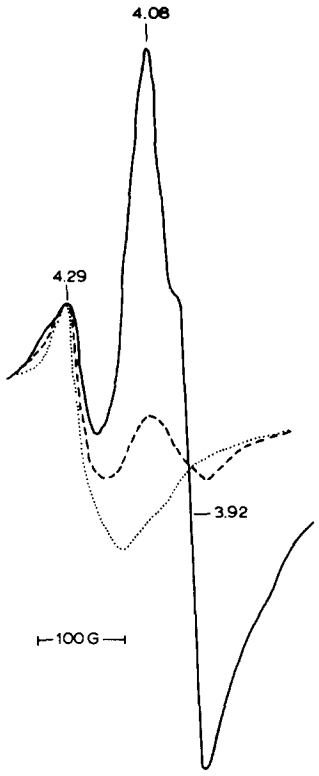

Fig. 1. The $g = 4$ region of the EPR spectrum of a BBY membrane preparation (1 mg Chl/ml (pH 6.0)) untreated (·····), following incubation with 0.8 mM NO in darkness (———) for 40 min and following illumination of the latter at 200 K (— — —). EPR conditions: temperature, 4.2 K; microwave power, 12.6 mW; microwave frequency, 9.42 GHz; modulation amplitude, 16 G.

line) shows that the $g = 4$ signal has almost entirely disappeared upon illumination at 200 K.

The $g = 4$ resonance can be restored in the illuminated sample by subsequent dark adaptation at elevated temperatures. When illumination is performed at 4.5 or 100 K, the resonance can be restored by subsequent warming in the dark at 240 K for 2–3 min. Recovery of the $g = 4$ signal in this case parallels the decay of a narrow free radical species ($\Delta H_{pp} = 10$–11 G) at $g = 2$ which is light-induced at low temperatures (see below). When illumination is performed at about 200 K, no significant narrow free-radical species is induced and the $g = 4$ signal can be restored only after incubating the sample at $T \geqslant 273$ K in darkness. Here, more stable donors are functioning, which require higher temperatures for recombination. Possible donors, at 200 K, include the oxygen-evolving complex, cytochrome *b*-559 (at [NO] $\leqslant 100$ μM), and, at high enough concentrations, NO itself (see Fig. 8).

The disappearance of the $g = 4$ signal upon illumination can be explained by various hypotheses: photodissociation of an NO adduct, reduction or oxidation of the species responsible for the $g = 4$ signal, or exchange coupling with the spin of a nearby electron acceptor or donor. The variability in the temperature of signal recovery as a function of the illumination temperature and the results of the next section would appear to eliminate the first possibility. In untreated BBY membranes, illumination at less than 120 K results in the formation of Q_A^- and the oxidation of the donor responsible for the narrow free radical. Subsequent dark adaptation at 240 K results in charge recombination faster than electron transfer to Q_B. Upon illumination at 200 K or above, Q_A^- formation is accompanied by oxidation of a more stable donor (e.g., O_2-evolving complex). Here, upon warming, electron transfer to Q_B is faster than recombination. Slow reoxidation of Q_B^- is required at room temperature to restore the $g = 4$ signal.

Binary oscillations of the $g = 4$ signal in chloroplasts

Treatment of spinach chloroplasts in the dark with NO also elicits a $g = 4$ EPR signal with characteristics similar to that observed in BBY preparations. Fig. 2 shows the evolution of this signal following successive cycles of illumination at 200 K followed by warming in the dark to either 240 or 273 K (third cycle only). Apart from small differences in signal shape, the amplitude undergoes prominent binary oscillations which are shown up to the fifth cycle. Binary oscillations of semiquinone concentration are a property of the two-electron gate of the acceptor side of PS II in previously dark-adapted chloroplasts [35,36]. It is likely that the oscillatory behavior of Fig. 2 is a reflection of this phenomenon, a conclusion that is supported by further EPR, Mössbauer and optical data presented in this and the companion paper [18].

Spinach chloroplasts and BBY membranes are known to be capable of electron transfer from Q_A to Q_B at 240 K [37,38]; however, replacement of quinol by quinone

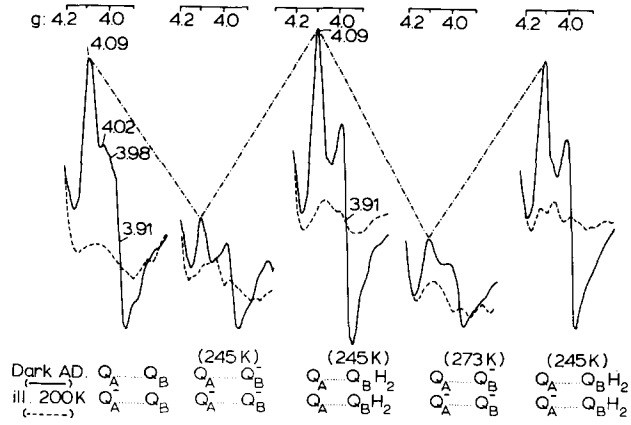

Fig. 2. Binary oscillations of the $g = 4$ EPR signal in spinach chloroplasts (2 mg Chl/ml (pH 7.5)) in the presence of 180 μM NO during successive illuminations (200 K, 3 min) of the reaction center, followed by warming in the dark (4 min 245 K or 30 s at 273 K) to allow secondary electron transfer to Q_B. The traces indicated by (———) are the dark spectra just prior to illumination at 200 K (— — —). The EPR detection conditions are as in Fig. 1.

in the Q_B site requires higher temperatures [17,39]. Indeed, warming to 273 K on the third cycle is required for continued oscillations, a reflection of the need to exchange quinol, Q_BH_2, for quinone. Failure to warm to 273 K at this point results in the loss of further oscillations. Also, fluorescence relaxation experiments under similar conditions (Ref. 18), but at room temperature, indicate that Q_A to Q_B electron transfer, functioning as a two-electron gate, is still operative in the presence of NO but occurs with lower rates. As the $g = 4$ species cannot be due to a quinone-NO complex, the periodic pattern of Fig. 2 is most readily explained by a magnetic interaction of the NO adduct with the unpaired spin on either of the semiquinones

The $g = 4$ signal in Fig. 2 is maximal in states Q_AQ_B and $Q_AQ_BH_2$. These are states having zero spin on the quinones. The signal is small when either one or both quinones are singly reduced. As shown in a subsequent section, the $g = 4$ signal arises from an $S = 3/2$ system. An exchange interaction between this spin and the $S = 1/2$ of either of the two singly reduced quinones should result in spin states with integer total spin which are either EPR-silent or give competely different resonances. In the state where both quinones are singly reduced, three interacting spins, 1/2, 3/2 and 1/2, will couple in a manner which will depend on the relative strength of the various exchange interactions. If the three possible exchange interactions are different, this coupling will result in a multitude of substates with half-integer spin and with weak EPR resonances extending over broad field limits and with different temperature dependencies. This probably explains why no obvious alternative resonances were observed in the state $Q_A^-Q_B^-$. Detection of such resonances would have provided additional direct evidence for an exchange interaction.

The data in this section rule out the possibility that the $g = 4$ species is an electron donor or acceptor, as such behavior would not explain the oscillation with period two in signal amplitude with each charge separation. The possibility that a negative charge on either or both of the quinones dissociates the NO is unlikely as one would expect such charge to enhance the binding of the electrophilic NO ligand. An additional argument against this hypothesis and in favor of magnetic interaction is provided by the experiment presented in Fig. 6 of the accompanying paper [18]. In this experiment, formation of the Fe(II)-NO adduct is shown to depress the amplitude of the Q_A^-Fe(II) EPR signal, consistent with an exchange-type interaction.

Mössbauer evidence for an interaction between the acceptor side Fe(II) and NO

An Fe(II) is located between Q_A and Q_B [10,14], which can interact by exchange coupling with the spin on either of the quinones in their semiquinone states

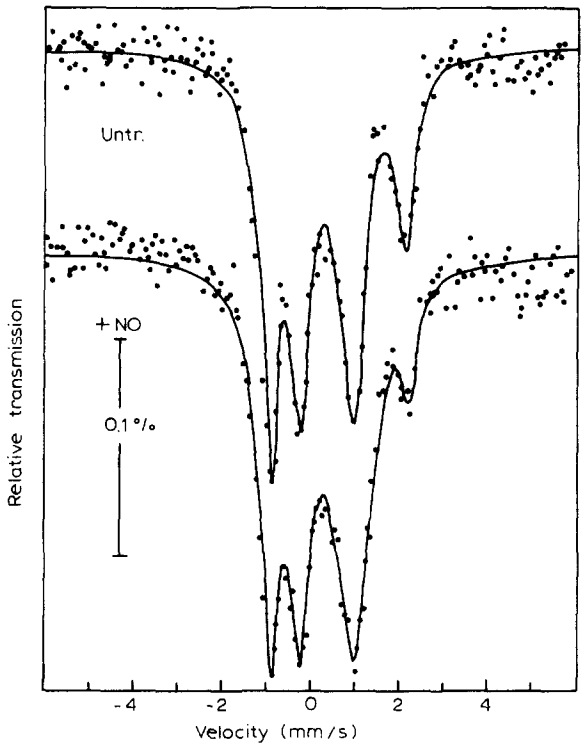

Fig. 3. Mössbauer spectra of a *C. reinhardtii* PS II core particle preparation (4.6 mg Chl/ml, pH 6.5, 150 K) untreated (upper) and following stirring in darkness for 30 min in a 100% NO atmosphere (lower). The continuous lines are computer simulations assuming Lorentzian lineshapes and independent linewidths.

[3,4,16]. High-spin Fe(II)-NO complexes exhibiting EPR resonances in the $g = 4$ region are well documented [19–25]. This and the above oscillatory data (Fig. 2) make the PS II acceptor-side Fe(II) a very likely candidate for the binding of NO. The Mössbauer spectrum of this non-heme iron at 150 K in PS II core particles from *Chlamydomonas* (pH 6.5) is shown in Fig. 3 (upper, the second and fourth peaks from the left). The only other iron component in these preparations (the first and third peaks from the left) is due primarily to low-spin Fe(III) cytochrome b-559 [6].

NO treatment of this material produces a $g = 4$ EPR signal with g values identical to those observed in the BBY preparations (not shown). Fig. 3 (lower) shows the effect on the Mössbauer spectrum of 30 min of stirring of the sample under an NO atmosphere. The rightmost Fe(II) peak decreases by over 60%, indicating that the NO adduct interacts with the iron in more than half the centers and that the new species has a different spectrum. The low-potential cytochrome *b*-559, present in the oxidized state, appears to be unaffected. The leftmost peak of the Fe(II) spectrum has not decreased appreciably. It is likely that the leftmost peak of the Fe(II)-NO spectrum coincides approximately in position with the left peak of the original Fe(II) doublet. The rightmost peak of the Fe(II)-NO spectrum probably falls in the vicinity of the righmost peak of the

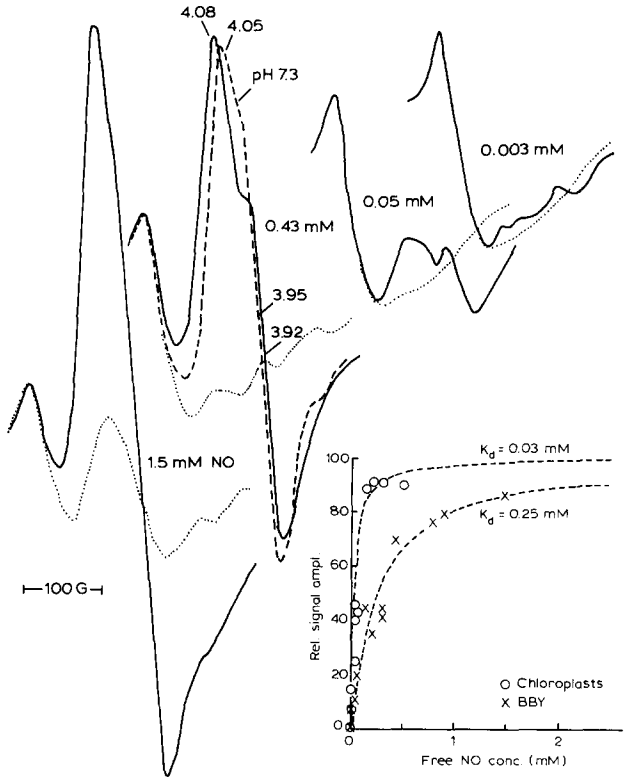

Fig. 4. Representative EPR spectra of BBY preparations (1 mg Chl/ml (pH 6.0) at the indicated NO concentrations in the dark (———) and following illumination at 200 K (· · · · · ·). The dashed line spectrum is from a sample at pH 7.3 (3.3 mg Chl/ml) treated with 560 μM NO and recorded under the same EPR conditions as the other spectra. Instrument settings as in Fig. 1. Lower right. Dependence of the $g = 4$ EPR signal on the NO concentration in spinach chloroplasts (o) and BBY preparations (x). Dashed traces are theoretical binding curves with the indicated K_d values, the only other adjustable parameter being the 100% level. Concentrations of NO above 1.5 mM could not be used as light-insensitive $g = 4$ signals appeared.

cytochrome, which now appears broader. There may not be strict conservation of the detectable area of the non-heme iron spectrum. Relaxation broadening may have decreased the intensity of the Fe(II) – NO spectrum. In any case it is clear that the acceptor-side non-heme iron is affected by the NO treatment.

In sum then, the similarity of the $g = 4$ EPR signal (Fig. 1) to those of other well established Fe(II)-NO complexes [19–25], the binary oscillations of the $g = 4$ signal (Fig. 2), the effect of the NO on the rate of Q_A-Q_B electron transfer (see Ref. 18), and the effect of NO on the Mössbauer spectrum of the acceptor-side Fe(II) (Fig. 3) all point to the conclusion that it is this iron which has formed the NO complex responsible for the $g = 4$ EPR signal.

Titration of NO binding to the non-heme Fe(II)

Fig. 4 shows a series of Fe(II)-NO spectra in BBY membranes at pH 6.0 at various NO concentrations. The spectrum at high and low NO concentrations show some difference in signal shape, suggesting the presence of two slightly different superimposed components having somewhat different binding affinities for NO. These could not be distinguished and the combined titration curve is shown with a K_d of 250 μM (Fig. 4, lower right). Also plotted are data points from a titration of the $g = 4$ signal in chloroplasts at pH 6.3. This titration shows much tighter binding of NO with a K_d of about 30 μM. Spinach chloroplasts show a higher rate of electron transfer between the quinones, Q_A and Q_B [40,41] than do the BBY membranes [39]. This difference probably arises from a lower concentration of quinone in the Q_B site in the latter. Spinach BBY membranes [42] also show a higher K_d for DCMU than do chloroplasts [43]. These differences may have a common origin with the difference in NO affinity for the iron.

Fig. 4 shows a representative spectrum of an NO-treated BBY preparation at pH 7.3 superimposed on a spectrum measured at pH 6.0. Two differences are observed. The integrated area of the spectrum, on a per chlorophyll basis, is several times smaller at pH 7.3 (discussed in the companion paper [18], Fig. 3). The spectrum at pH 7.3 is also narrower, indicating a more axial environment at high pH (see next section). The resolution of the spectra is not sufficient to determine whether or not this more axial component is the same as that observed at high NO concentrations at pH 6.0 (Fig. 4). A difference in protonation state could be responsible for the two species. A similar broadening has been observed in the EPR spectrum of Fe(III) upon lowering the pH [39].

Effects of NO on the PS II electron donor side

Reversible effect of NO on EPR Signal II_{dark}

Fig. 5a (continuous line) shows EPR Signal II_{dark} [44] present in a BBY sample at pH 7.3, bubbled gently in darkness at 4 °C with 5 ml N_2 gas. Figs. 5b and c (continuous line) show the same region of the spectrum in two like samples that were bubbled with a 5 ml mixture of N_2 and NO, resulting in 100 μM dissolved free NO. Signal II is absent from the latter samples. As discussed below, the high-field tail of the signal is due to free dissolved NO. Illumination at 200 K results in a 2.5-fold increase in Signal II in the absence of NO (Fig. 5a). In the presence of NO (Fig. 5b), similar illumination conditions result only in low-level generation of the narrow free-radical signal. 1-min evacuation in the EPR tube of sample (c) while shaking on a vortex mixer at 0 °C in the dark removes NO and restores the Signal II practically to the control level (Fig. 5c, dashed line). This restoration of Signal II shows that its loss in the presence of NO is not due to either damage or to chemical reduction.

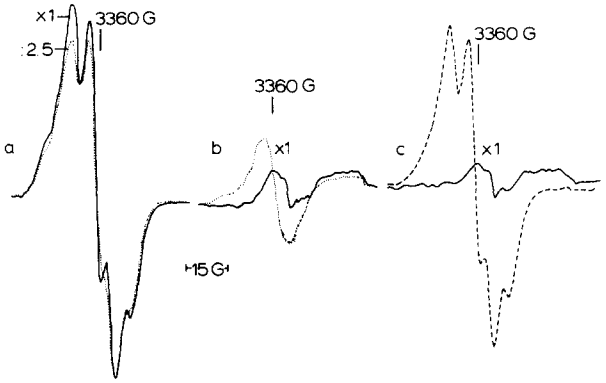

Fig. 5. Effect of NO on EPR Signal II. BBY membranes (3.3. mg Chl/ml, 100 mM Hepes-NaOH(pH 7.3)) were stirred under an N_2 atmosphere for 30 min at 4°C and then slowly bubbled (about 1 ml/min) with 5 ml (a) pure N_2; (b and c) approx. 5% NO in N_2. The final concentrations of NO were, respectively, 0, 130 μM and 100μM for (a), (b) and (c). The spectra indicated are those in the dark (———) followed by 200 K illumination (a, b, · · · · · ·) and after thawing while pumping off NO in the EPR tube (c, — — —). Instrument settings: 10 K; microwave power, 36 dB; modulation amplitude, 4 G; microwave frequency, 9.42 GHz.

The above effects can be explained if we assume that NO binds to a site on or near the Signal II species so that the spin = 1/2 of NO reacts by exchange interaction with the spin = 1/2 in the oxidized state of Signal II to form $S = 0$ or, less likely, an $S = 1$ spin state which is EPR-silent. In order to explain the observation that there is no increase in Signal II upon illumination at 200 K in the presence of NO, we must assume either that NO binds with high affinity nearby the reduced precursor, D, to Signal II or that NO can diffuse at 200 K to bind to D^+ or donate electrons to $P680^+$.

To test whether Mn could be the binding site of NO we have examined the effect of NO treatment on two preparations lacking 2–3 Mn of the oxygen-evolving complex yet capable of generating Signal II dark at normal levels. A membrane preparation from *Scenedesmus* mutant LF-1 (1.5–2Mn/RC, [31]) and a PS II particle preparation from *Chlamydomonas* (about 1 Mn/RC, [33]) both show (Fig. 6 complete disappearance of Signal II_{dark} upon treatment with NO.

Titration of the NO effect on Signal II_{dark}

Fig. 7 shows Signal II spectra in the dark following treatment of BBY membranes with variable concentrations of NO. Similar behavior is observed in spinach chloroplasts. Titration of the disappearance of Signal II in both BBY membranes and spinach chloroplasts shows a K_d approx. 3 μM, much lower than that for the appearance of the $g = 4$ EPR signal (Fig. 4).

A broad contribution becomes increasingly apparent at high NO concentrations (Fig. 7). This signal is light insensitive (dotted trace) and corresponds to free NO in solution (see dashed trace). This signal has been used to determine the concentration of free NO in the titrations of the $g = 4$ signal and of the Signal II disappearance. The measurement of the NO concentration by this method is limited by the signal to noise ratio, to a minimum of 60 μM. At lower concentrations, the NO concentration was calculated from the partial pressure of NO in an N_2 atmosphere and the solubility of NO in water.

Effect of NO on other donor-side components

Mössbauer studies (not shown) on BBY preparations indicated that stirring in the dark under an atmosphere of NO resulted in the conversion of all of the high-potential (and therefore reduced) low-spin cytochrome *b*-559 to an $S = 1/2$ state. There is either formation of a cytochrome *b*-559-NO adduct or oxidation of the cytochrome by NO. Consistent with a modification of cytochrome *b*-559 is the observation that illumination of 500 μM NO-treated BBY samples at 80 K elicited a strong narrow free radical donor signal accompanied by the disappearance of the $g = 4$ Fe(II)-NO EPR signal, instead of the usual donor-side high-potential $g = 3$ ferricytochrome *b*-559. Whenever the narrow free radical appeared upon illumination between 4.2 and 120 K in the presence of NO, raising the temperature, in the dark, to 240 K resulted in charge recombination. The

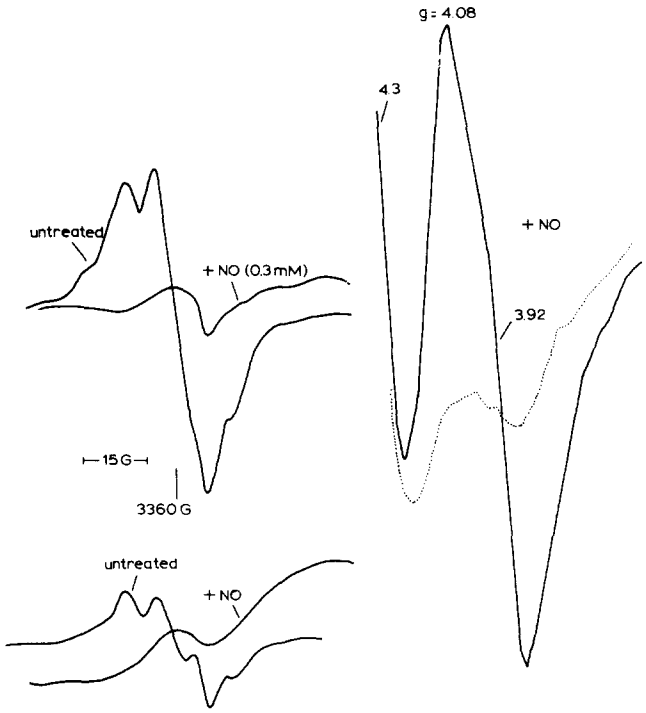

Fig. 6. Upper. Dark EPR spectra of *Scenedesmus* LF-1 membranes (2.9 mg Chl/ml, 5 mM MES (pH 6.0)) in the $g = 2$(left) and $g = 4$(right) regions following treatment with 300 μM NO. Instrument settings: Left $T = 10$ K; microwave power, 36 dB; modulation amplitude, 5 G. Right T = 4.2 K; microwave power, 12 dB; modulation amplitude, 32 G. Similar results were obtained with wild-type *Scenedesmus*. Lower. Effect of 400 μM NO on the EPR spectrum of Signal II in *Chlamydomonas* PS II core particles (0.7 mg Chl/ml, 3.5 mM Mes (pH 6.5). Instrument settings as in Fig. 5.

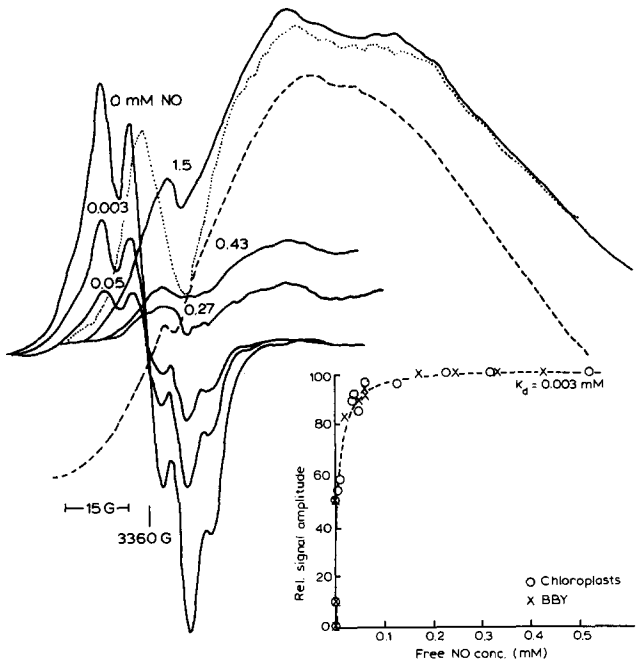

Fig. 7. Effect of NO, at the indicated concentrations, on the amplitude of Signal II dark (D^+) in BBY membranes (1 mg Chl/ml (pH 6.0)). The spectra indicated are those in the dark (———). For the sample treated with 1.5 mM NO the spectrum following subsequent illumination at 200 K is also indicated (· · · · · ·). The dashed trace shown for comparison is the spectrum of the suspension medium treated with NO at a final concentration of 1.8 mM. The EPR instruments settings are as in Fig. 5. Inset. Dependence of percent decrease in Signal II on the concentration of NO in spinach cloroplasts (o) and BBY membranes (x).

narrow free radical would disappear and the $g = 4$ acceptor-side EPR signal would reappear. This protocol could be repeated several times. Illumination of NO-treated samples at 200 K gave little narrow free radical, regardless of the NO concentration. The state $S2$ multiline EPR signal of the oxygen-evolving complex, induced upon illumination of BBY preparations at 200 K, decreased as the NO concentration increased above 300 μM and was not detectable above 1 mM. Illumination under these conditions always resulted in the disappearance of the $g = 4$ EPR signal, indicating that charge separation was occurring. It is likely that under these conditions NO acts as a donor.

Blockage of charge recombination by NO

If NO were to act as an electron donor to the reaction center, then in the presence of DCMU, one would expect to see blockage of Q_A^- oxidation following its photoreduction. This prediction is borne out by the experiment of Fig. 8, in which increasingly elevated concentrations of NO produce an increasing concentration of centers which show a stabilized Q_A^- following a saturating light flash in the presence of DCMU. The fluorescence yield at 5 ms after the actinic flash corresponds to the maximum flash yield of Q_A^- in the presence of 10 μM DCMU. At 11 s after the flash, the fluorescence yield is about 5% of the maximum in the absence of NO. As the NO concentration is increased, the yield at 11 s increases, attaining about half the centers blocked at about 30 μM NO (allowing for the non-linear dependence of Q_A^- on the fluorescence yield [45], Fig. 8, inset). The blockage by NO is pH-independent in the range 6.3–7.4. This pH-independence distinguishes this phenomenon from the acceptor-side binding of NO to the iron, the rate of which is pH-dependent [18]. We conclude that the blockage of charge recombination by NO is most likely a donor-side effect alone. This experiment was not carried out beyond 50 μM NO because of excessive fluorescence quenching by NO.

While consistent with outright electron donation by NO, we cannot exclude the possibility that blockage of charge recombination occurs via stabilization by NO of an oxidized donor whose EPR spectrum would be obscured by exchange coupling. The concentration observed in the fluorescence experiment, for blockage of one-half the centers, is an order of magnitude less than that observed for blockage of the light-induced formation of the multiline signal at 200 K in BBY prepara-

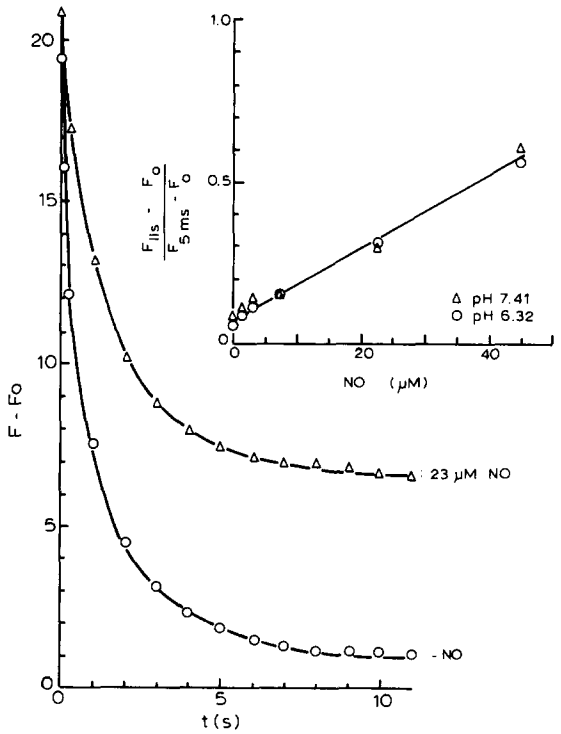

Fig. 8. Kinetics of relaxation of the fluorescence yield in spinach chloroplasts following a saturating flash in the presence and absence of NO. Spinach chloroplasts were suspended at 10 μg Chl/ml in 50 mM sodium phosphate (pH 6.33), containing 0.3 M sorbitol, 10 mM NaCl, 5 mM $MgCl_2$ and 10 μM DCMU. Inset. Dependence of the fluorescence yield at 11 s normalized to that at 5 ms following a saturating flash and at various NO concentrations. Spinach chloroplasts were used under the same conditions, but at pH 6.33 (o); and 7.41(Δ).

tions. This difference likely arises from the higher temperature at which the fluorescence experiment was performed −298 K (Fig. 8) versus 200 K.

Discussion

Interpretation and characteristics of the Fe(II)-NO $g = 4$ EPR signal

In all reported cases of high spin Fe(II)-NO complexes exhibiting the $g = 4$ EPR signal, the ground state of the system has a spin of 3/2 [19–25]. This is certainly the case as well for the PS II acceptor-side Fe(II)-NO adduct. The spin 3/2 state is the resultant of an antiferromagnetically spin-coupled pair, NO ($S_1 = 1/2$) and Fe(II)($S_2 = 2$). Charge delocalization in this system is, however, likely, and the Fe(II)-NO complex is more formally described as a $3d^7$ system.

The magnetic properties of an isolated $S = 3/2$ state can be described by the following Hamiltonian:

$$\mathcal{H} = D(S_z^2 - 5/4) + E(S_x^2 - S_y^2) + g\mu_B \boldsymbol{S}\cdot\boldsymbol{H} \qquad (1)$$

where D and E are a measure of axial and rhombic crystal field distortion and $\boldsymbol{H}$ is the applied magnetic field in the EPR experiment. Explicit approximate solutions of this hamiltonian are discussed in Ref. 21. Here we recall briefly the results relevant to our spectra. When the D term dominates in Eqn. (1), the $S = 3/2$ system is approximately described as two doublets with S_z values of $\pm 1/2$ and $\pm 3/2$ separated in energy by about $2D$. For small E/D values, only the $\pm 1/2$ doublet is EPR active and the g values are approximated as follows:

$$\begin{aligned} & E/D < 0.15 && E/D < 0.03 \\ & g_x \approx g_0\left[2 - 3(E/D) - 3/2(E/D)^2\right] && \approx g_0[2 - 3(E/D)] \\ & g_y \approx g_0\left[2 + 3(E/D) - 3/2(E/D)^2\right] && \approx g_0[2 + 3(E/D)] \\ & g_z \approx g_0[1 - 3(E/D)^2] && \approx g_0 \end{aligned} \qquad (2)$$

g_0 is the free-ion g value, generally equal to 2.0. The resonances g_x and g_y, centered around $g = 4$, are very intense, while the g_z resonance at 2 is difficult to observe, particularly in the present case, where the $g = 2$ region is dominated by signals due to other paramagnetic species. In the calculation of the g values, the position of the impurity peak at $g = 4.29$ was taken as an internal reference.

The spectrum in Fig. 1 with $g_x = 3.92$ and $g_y = 4.08$ indicates an E/D value of 0.013. Due to the inhomogeneous nature of the EPR spectra in BBY preparations at pH 6.0, the apparent E/D value at high NO concentrations is somewhat smaller and at low NO concentrations somewhat higher (Fig. 4). The E/D value, corresponding to the spectrum at pH 7.3 in Fig. 4 ($g_x = 3.95$, $g_y = 4.05$) is 0.008, indicating a more axial environment at high pH. The spectrum of the chloroplast preparation, Fig. 2, in the dark (state Q_AQ_B) consists of an outer component with $g_x = 3.91$ and $g_y = 4.09$, corresponding to $E/D = 0.015$ and a weak inner component with $g_x = 3.97$ and $g_y = 4.02$, implying $E/D \approx 0.004$. It is interesting that the spectrum in the $Q_AQ_BH_2$ state is more homogeneous, consisting of only the outer component. This provides at least a partial explanation as to why the signal intensity appears to be enhanced in the latter state. To what extent this reflects local conformational changes, protonation-deprotonation events or dissociation of the secondary quinone is not at present clear. Measurements of the electron transfer rate from Q_A to Q_B (see accompanying paper [18]) as a function of flash number in the presence of NO show a minor slowing of the electron transfer rate following the first saturating flash, compared to the control rate in the absence of NO. On the second and following flashes the rates are slowed by more than a factor of 10. The increased rhombicity of the Fe(II)-NO signal following the second charge separation may be related to this observation. Both may reflect a deprotonated state of the protein, associated with the formation of $Q_AQ_BH_2$ or $Q_AQ_BH^-$.

Other examples of Fe(II)-NO adducts such as soybean lipoxygenase [22,23] and the protocatechuate dioxygenases [20,21] also show heterogeneity in the iron environments as evidenced by a heterogeneity in E/D of the Fe(II)-NO EPR signals. These show a dependence on pH, on the concentration of NO, on the presence of organic solvents and on the presence of substrate, which either compete with NO for binding to the iron or bind at the same time. Aside from outright competition with NO for binding to the non-heme iron, the origin of these perturbations is not yet known, though protonation-deprotonation events and changes in polarization of other iron-ligand bonds have been suggested.

The acceptor-side non-heme iron of spinach chloroplasts demonstrates a K_d for NO of 30 μM, nearly an order of magnitude lower than that (250 μM) for NO in BBY membrane preparations. The BBY Fe(II)-NO EPR spectrum at pH 7.3–7.5 is also more axial than that of the chloroplasts. Previous measurements have indicated other differences between the iron environments in these two materials. The dissociation constant for DCMU is considerably lower in spinach chloroplasts [43] than in BBY preparations [42]. Measurement of the Fe(III) EPR spectrum indicated that BBY preparations had a lower percentage of the Q_B sites occupied [17]. Consistent with this observation is the 10-fold lower rate of electron transfer from Q_A^- to Q_B in the BBY preparations [39] than in chloroplasts [40,41]. One is tempted to attribute these differences in K_d and in E/D to the

difference in the concentration of quinone in the Q_B site. We also note that the intensity of the $g = 4$ resonance is, on a per chlorophyll basis, more than an order of magnitude stronger than the $g = 8.1$ peak of the Fe(III). This observation is, however, in accord with theoretical expectations. The systematic study of the above effects will be the subject of a separate investigation.

Considering its ability to act as both an electron donor and acceptor [46], it is not unexpected that NO can be oxidized by the highly oxidizing electron donor side of the PS II reaction center. What is more surprising is the NO-induced disappearance of the EPR Signal II arising from D^+, a tyrosine free radical [47–49]. The loss of EPR Signal II is reversed upon removal of NO in vacuo, indicating that the disappearance of this signal is most likely by exchange coupling in the immediate environment of D^+. NO might bind directly to D^+ or to a metal center nearby. Considering the weak effect of Mn on the power saturation characteristics of D^+ [44] compared to Z^+ [50] at room temperature, it would seem unlikely that the binding of NO to Mn is responsible for the disappearance of Signal II_{dark}. Consistent with this argument is the observation that reaction center and membrane preparations depleted of 1/2 to 3/4 of the Mn associated with the O_2-evolving site did not eliminate the NO-induced disappearance of EPR Signal II (Fig. 6). Of the other known metal centers, the non-heme iron is eliminated by its much higher K_d for NO (compare Figs. 4 and 7). Cytochrome *b*-559 seems unlikely, as no EPR signals are observed in the $g = 2$ region, arising from an NO-low spin Fe(II) heme adduct. There is therefore insufficient evidence, at this point, to assign a binding site for the effect of NO on Signal II_{dark}.

Considering that NO can bind as a ligand to many heme proteins, it is reasonable to expect that other common ligands to heme iron might bind to the PS II iron as well. Measurements of the rate of electron transfer between Q_A and Q_B, an indicator of ligand binding to the iron (see accompanying paper [18]), showed that NO slowed this rate by a factor of at least 10. CO at 100 μM had no effect. However, CN^-, at 30 mM had quite a large effect on the rate of electron transfer, showing kinetic modifications quite similar to those of NO. These included a lesser effect on the first flash and a much larger slowing on the second and subsequent flashes. The origin of the slowing of the electron transfer will be discussed in Ref. 18.

Acknowledgements

The authors would like to thank Dr. A. Kostikas for valuable help during the early stages of this work and Dr. Mark Nelson for helpful discussion.

References

1 Dutton, P.L. Leigh, J.S. and Reed, D.W. (1973) Biochim. Biophys. Acta 212, 654–664.
2 Feher, G. and Okamura, M.W. (1978) in The Photosynthetic Bacteria (Clayton, R., ed.), pp. 349–386, Plenum Press, New York.
3 Nugent, J.H.A., Diner, B.A. and Evans, M.C.W. (1981) FEBS Lett. 124, 241–244.
4 Rutherford, A.W. and Zimmermann, J.L. (1984) Biochim. Biophys. Acta 767, 168–175.
5 Boso, B., Debrunner, P., Okamura, M.Y. and Feher, G. (1981) Biochim. Biophys. Acta 638, 173–177.
6 Petrouleas, V. and Diner, B.A. (1982) FEBS Lett. 147, 111–114.
7 Petrouleas, V. and Diner, B.A. (1980) in Advances in Photosynthesis Research (Sybesma, C ed.), Vol. I, pp. 195–198, Martinus Nijhoff/Dr.W. Junk Publishers, Dordrecht.
8 Dismukes, G.C., Frank, H.A., Friesner, R. and Sauer, K. (1984) Biochim. Biophys. Acta 764, 253–271.
9 Michel, H. and Deisenhofer, J. (1986) in Photosynthesis III, Encyclopedia of Plant Physiology New Series, Vol. 19 (Staehelin, L.A. and Arntzen, C.J., eds), pp. 371–381, Springer Berlin.
10 Allen, J.P., Feher, G., Yeates, T.O. Komiya, H. and Rees, D.C. (1988) Proc. Natl. Acad. Sci. USA 85, 8487–8491.
11 Hearst, J.E. (1986) in Photosynthesis III in Encyclopaedia of Plant Psychology, New Series, Vol. 19 (Staehelin, L.A. and Arntzen, C.J. eds.), pp. 382–389, Springer, Berlin.
12 Deisenhofer, J., Epp, O., Miki, K., Huber, R. and Michel, H. (1985) Nature 318, 618–624.
13 Trebst, A. (1986) Z. Naturforsch. 41c, 240–245.
14 Michel, H. and Deisenhofer, J. (1988) Biochemistry 27, 1–7.
15 Petrouleas, V. and Diner, B.A. (1986) Biochim. Biophys. Acta 849, 264–275.
16 Beijer, C. and Rutherford, A.W. (1987) Biochim. Biophys. Acta 890, 169–178.
17 Diner, B.A. and Petrouleas, V. (1987) Biochim. Biophys. Acta 895, 107–125.
18 Diner, B.A. and Petrouleas, V. (1990) Biochim. Biophys. Acta, 1015, 141–149.
19 Rich, P.R., Salerno, J.C., Leigh, J.S. and Bonner, W.D. (1978) FEBS Lett. 93, 323–326.
20 Arciero, D.M., Lipscomb, J.D., Huynh, B.H., Kent, T.A. and Münck, E. (1983) J. Biol. Chem. 258, 14981–14991.
21 Arciero, D.M., Orville, A.M. and Lipscomb, J.D. (1985) J. Biol. Chem. 260, 14035–14044.
22 Salerno, J.C. and Siedow, J.N. (1979) Biochim. Biophys. Acta 579, 247–251.
23 Nelson, M.J. (1987) J. Biol. Chem. 262, 12137–12142.
24 Bernhardt, F.H., Gersonde, K., Twitter, H., Wende, P., Bill, E., Trautwein, A.X. and Pfleger, K. (1982) in Oxygenases and Oxygen Metabolism (Nozaki, M., Yamamoto, S., Ishima, Y., Coon, M., Ernster, L. and Estabrook, R., eds.), pp. 63–77, Academic Press, New York.
25 Nocek, J.M., Kurtz, D.M., Sage, J.T., Debrunner, P.G., Maroney, M.J. and Que, L. (1985) J. Am. Chem. Soc. 107, 3382–3384.
26 Slappendal, S., Aasa, R., Malmström, B.G., Verhagen, J., Veldink, G.A. and Vliegenthart, J.F.G. (1982) Biochim. Biophys. Acta 708, 259–265.
27 Ford, R.C. and Evans, M.C.W. (1983) FEBS Lett. 160, 159–164.
28 Rutherford, A.W., Zimmermann, J.L. and Mathis, P. (1984) FEBS Lett. 165, 156–162.
29 Berthold, D.A., Babcock, G.T. and Yocum, C.F. (1981) FEBS Lett. 134, 231–234.
30 Metz, J.G. Wong, J. and Bishop, N.I. (1980) FEBS Lett. 114, 61–66.
31 Metz, J.G. and Seibert, M. (1984) Plant Physiol. 76, 829–832.
32 Avron, M. (1960) Biochim. Biophys. Acta 40, 257–272.

33 Diner, B.A. and Wollman, F.A. (1980) Eur. J. Biochem. 110, 521–526.
34 Joliot, P., Béal, D. and Frilley, B. (1980) J. Chim. Phys. 77, 209–216.
35 Bouges-Bocquet, B. (1973) Biochim. Biophys. Acta 314, 250–256.
36 Velthuys, B.R. and Amesz, J. (1974) Biochem. Biophys. Acta 333, 85–94.
37 Joliot, A. (1974) Biochim. Biophys. Acta 357, 439–448.
38 De Paula, J.C., Innes, J.B. and Brudvig, G.W. (1985) Biochemistry 24, 8114–8120.
39 Petrouleas, V. and Diner, B.A. (1987) Biochim. Biophys. Acta 893, 126–137.
40 Bouges-Bocquet, B. (1973) Biochim. Biophys. Acta 292, 772–785.
41 Bowes, J.M. and Crofts, A.R. (1980) Biochim. Biophys. Acta 590, 373–384.
42 Wraight, C. (1985) Biochim. Biophys. Acta 809, 320–330.
43 Diner, B.A. and Petrouleas, V. (1987) Biochim. Biophys. Acta 893, 138–148.
44 Babcock, G.T. and Sauer, K. (1973) Biochim. Biophys. Acta 325, 483–503.
45 Joliot, A. and Joliot, P. (1964) C. R. Acad. Sci. Paris 258, 4622–4625.
46 McCleverty, J.A. (1979) Chem. Rev. 79, 53–76.
47 Barry, B.A. and Babcock, G.T. (1987) Proc. Natl. Acad. Sci. USA 84, 7099–7103.
48 Debus, R.J., Barry, B.A., Babcock, G.T. and McIntosh, L. (1988) Proc. Natl. Acad. Sci. USA 85, 427–430.
49 Vermaas, W.F.J. Rutherford, A.W. and Hansson, O. (1988) Proc. Natl. Acad. Sci. USA 85, 8477–8481.
50 Yocum, C.F. and Babcock, G.T. (1981) FEBS Lett. 130, 99–102.